Flux-weakening Characteristics of Non-sinusoidal Back-EMF PM Machines in Brushless DC and AC Modes

Z. Q. Zhu [1], J. X. Shen [2], and D. Howe [3]

[1] *Department of Electronic and Electrical Engineering, University of Sheffield, Z.Q.Zhu@sheffield.ac.uk*
[2] *Department of Electronic and Electrical Engineering, University of Sheffield*
[3] *Department of Electronic and Electrical Engineering, University of Sheffield*

Abstract

Recently, the application of surface-mounted magnet brushless machines to EVs/HEVs is extensively researched. In this paper, the performance of such kind of brushless motor which has a trapezoidal back-emf waveform when operated in BLDC and BLAC modes is evaluated, in both constant torque and flux-weakening regions, assuming (a) the same torque, (b) the same peak current, and (c) the same rms current. It is shown that although the motor has an essentially trapezoidal back-emf waveform, the output power and torque when operated in the BLAC mode in the flux-weakening region are significantly higher than that can be achieved when operated in the BLDC mode due to the influence of the winding inductance and back-emf harmonics.

Keywords

brushless ac, brushless dc, commutation advance, flux weakening, electric vehicle, permanent magnet machine

1. INTRODUCTION

Permanent magnet (PM) brushless machines having an interior-magnet rotor [Jahns, 1987] are widely accepted for EV/HEV applications for their excellent flux-weakening performance and high torque density. Indeed, they have been successfully used in the Toyota HEV system. In contrast, PM brushless machines a surface-mounted magnet rotor are often considered to have limited flux-weakening capability due to low winding inductance, potential irreversible demagnetization, as well as no reluctance torque. However, it was shown in [Soong et al., 1994] that if the machine can be designed to have per-unit d-axis winding inductance, a surface-mounted magnet machine can, at least theoretically, have infinite flux-weakening capability, as it has been proved experimentally in [Zhu, 2003] and successfully used for EVs/HEVs [Chan et al., 1994]. Surface-mounted magnet brushless machines having a fractional number of slots per pole and concentrated stator windings are attractive since they have shorter end-windings and, hence, a lower copper loss and a shorter overall axial length. Hence, they have the potential of high efficiency and high torque density, and are most suitable for applications which require short axial length, such as in-hub wheel motors [Chan et al., 1994]. Alternate teeth wound fractional-slot PM brushless machines [Chan et al., 1994; Ishak et al., 2005; Ishak et al., 2006] are particularly favoured since they can easily achieve a per-unit winding inductance and hence high flux-weakening capability, in addition to high torque density. Further, in such machines each phase is isolated physically and magnetically, which significantly improves its fault-tolerant capability. Therefore, they are eminently suitable for EV/HEV applications [Chan et al., 1994; El-Refaie et al., 2005; El-Refaie et al., 2006]. In addition, it is well-known that a fractional-slot machine exhibits low cogging torque [Zhu et al., 2000]. It is shown in [Zhu et al., 2002 and 2004] that the stator iron loss of surface-mounted magnet brushless machines can be significantly lower than that of interior-magnet brushless machines in the flux-weakening operation region, while the irreversible demagnetization withstand can remain high [Zhu et al., 2004], although the issue of rotor magnet eddy current loss should be considered [Atallah et al., 2000; Ishak et al., 2005].

PM brushless motors are generally classified according to their back-emf waveform, as being either sinusoidal or trapezoidal back-emf machines, as well as by their control strategy, which is usually classified as being either brushless DC (BLDC), in which case the phase current waveforms are essentially rectangular, or brushless AC (BLAC), in which case the phase current waveforms are essentially sinusoidal. Thus, in order to minimize torque pulsations, a machine with a trapezoidal back-emf waveform should be operated in BLDC mode, while a machine with a sinusoidal back-emf waveform should be operated in BLAC mode. For surface-mounted magnet, trapezoidal back-emf machines, maximum torque per ampere and extended speed operation can realized by advancing the commutation angle for both 2-phase, 120° and 3-phase, 180° BLDC conduction modes, as reported in [Jahns, 1984; Safi et al., 1995].

For sinusoidal back-emf machines, it is relatively easier to realize maximum torque per ampere control and extended speed operation since the optimal relationship between d- and q-axis currents can be analytically determined by employing vector control and flux-weakening control strategies [Jahns, 1987; Morimoto et al., 1994]. However, in practice, it is inevitable that harmonics exist in the back-emf waveform. Various design features may be employed to obtain a sinusoidal back-emf waveform. For example, the stator slots and/or rotor magnets may be skewed, a distributed stator winding may be employed, the magnets might be appropriately shaped or magnetised, etc. However, while such methods reduce the harmonic content in the back-emf waveform, they also reduce the average torque and increase manufacturing complexity and cost. Therefore, a machine with a non-sinusoidal back-emf waveform may be operated in BLAC mode [Liu et al., 2006], although its performance, in terms of efficiency and torque ripple, for example, may then be compromised.

In this paper, the performance of a motor having surface-mounted magnets and a trapezoidal back-emf waveform when operated in both BLDC and BLAC modes, Figure 1, is evaluated theoretically and experimentally, with particular reference to the flux-weakening performance. Hence, it is a fundamental study for the application to EV/HEV. The paper is organized as follows. Following the introduction, the torque capability of a motor having a trapezoidal back-emf waveform in both BLDC and BLAC modes is compared analytically in section 2. The flux-weakening performance is reported in sections 3 and 4 for BLDC and BLAC operation modes, respectively. The torque, power, efficiency and speed characteristics, in both constant torque and flux-weakening regions, are compared in section 5, assuming (a) the same torque, (b) the same peak current, and (c) the same rms current. The conclusions are given in section 6. To complement this investigation, the performance of a motor having interior magnets and a sinusoidal back-emf waveform when operated in BLDC and BLAC modes is compared in a companion paper [Zhu et al., 2006].

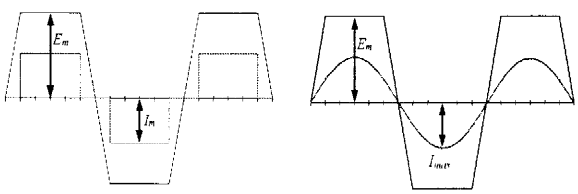

(a) BLDC (b) BLAC

Fig. 1 Schematic illustrating BLDC and BLAC operation of PM motor having trapezoidal back-emf waveform (below base-speed)

2. THEORETICAL COMPARISON OF TORQUE CAPABILITY

It is well known that if both the phase current and back-emf waveforms are ideal, as shown in Figure 1 (a), i.e. the back-emf waveform is trapezoidal with a flat top of at least 120° elec., and the current waveform is rectangular with a conduction angle of 120° elec., the electromagnetic torque of a BLDC motor will be ripple free, and can be expressed as:

$$T_{m\_BLDC} = \frac{2E_m I_m}{\Omega} = \frac{2pE_m I_m}{\omega} \tag{1}$$

where p is the number of pole-pairs, and Ω and ω are the mechanical and electrical angular velocity, respectively. Both the phase current and back-emf waveforms are rich in harmonics, as listed in Table 1, interaction between current and back-emf harmonics of the same order resulting in electromagnetic torque. The relative magnitudes of the component torques are also given in Table 1. From Table 1, it can be seen that:

(1) There are no third or other triplen harmonics in the phase current waveforms of a machine with a star-connected winding. However, other high order harmonics are significant.

(2) The most significant harmonic in the phase back-emf waveform is the third harmonic, higher harmonics being relatively low. However, the third-harmonic back-emf does not contribute to the production of electromagnetic torque.

(3) The electromagnetic torque results predominantly from the interaction between the fundamental components of the phase back-emfs and currents.

Table 1 Harmonics in idealised back-EMF and phase current waveforms of BLDC machine, and electromagnetic torque due to interaction harmonics of same-order

Order of harmonic (v)	Amplitude of back-emf harmonic (E_{mv}/E_m)	Amplitude of phase current harmonic (I_{mv}/I_m)	Torque due to harmonics of same-order (T_{mv}/T_m)
1	121.6%	110.3%	100.6%
3	27.0%	0	0
5	4.9%	-22.1%	-0.8%
7	-2.5%	-15.8%	0.3%
…	…	…	…

The electromagnetic torque in BLAC mode when the motor has a non-sinusoidal back-emf waveform can be expressed as:

$$T_{m\_BLAC} = \frac{3E_{m1}I_{\max}}{2\Omega} = \frac{3pE_{m1}I_{\max}}{2\omega} \qquad (2)$$

where E_{m1} is the amplitude of fundamental back-emf. The torque and current of a trapezoidal back-emf motor when operated in ideal BLDC and BLAC modes is given in Table 2. In BLAC mode, three cases are considered, viz. (a) the same torque, (b) the same peak current, and (c) the same RMS current as in BLDC mode.

Table 2 Current and torque of trapezoidal back-EMF motor in BLDC and BLAC modes

Amplitude of 120°-trapezoidal back-emf waveform		E_m		
BLDC mode	Amplitude of rectangular phase current waveform	I_m		
	Electromagnetic torque	$2E_m I_m / \Omega$		
BLAC mode	Amplitude of sinusoidal phase current waveform, I_{max}	$1.096I_m$	I_m	$1.155I_m$
	Electromagnetic torque	$2E_m I_m / \Omega$	$1.825E_m I_m / \Omega$	$2.107E_m I_m / \Omega$
	Condition	Same torque in BLDC mode	Same peak current as in BLDC mode	Same RMS current as in BLDC mode

It can be seen that to produce the same torque, the amplitude of the phase current in BLAC mode is 9.6% higher than that for the BLDC mode, while for the same peak current the torque which results in BLAC mode is 17.5% lower. For the same RMS current, i.e. the same copper loss, the phase current in BLAC mode can be increased by 15.5%, which results in the torque being increased by 10.7%.

3. FLUX-WEAKENING CONTROL AS BLDC DRIVE

To ease the investigation, a low power, 3-phase, 6-pole, 18-slot, surface-mounted PM brushless motor whose specification is given in Table 3, and which has a full-pitched overlapping stator winding, is considered. The phase back-emf waveforms are approximately trapezoidal, as shown in Figure 2, which also shows the measured third-harmonic voltage between the star-point and neutral. The DC link voltage is 200V, and the rated peak phase current for BLDC operation is I_m = 3.30A.

Flux-weakening control of a BLDC motor is achieved by advancing the commutation, measured torque-speed curves which result with different commutation advance angles being shown in Figure 3 (a), from which the optimal commutation advance angle for maximum torque at any speed is obtained, Figure 3 (b).

Table 3 Specification of BLDC motor

Number of poles:	6	Number of slots:	18
Winding:	Overlapping	Stator skew:	1 slot-pitch
Magnets:	Surface-mounted sintered ferrite	Self- & Mutual-inductances:	20.68mH, -2.81mH
Phase resistance:	3.37 ohm	Rated speed:	830rpm
DC link voltage:	200 V	Rated torque:	4.5Nm
Fundamental back-emf constant (k_{Em1}):		287.3 mV/(elec-rad/s)	
3rd harmonic back-emf constant (k_{Em3}):		64.5 mV/(elec-rad/s)	
5th harmonic back-emf constant (k_{Em5}):		15.6 mV/(elec-rad/s)	
7th harmonic back-emf constant (k_{Em7}):		2.5 mV/(elec-rad/s)	

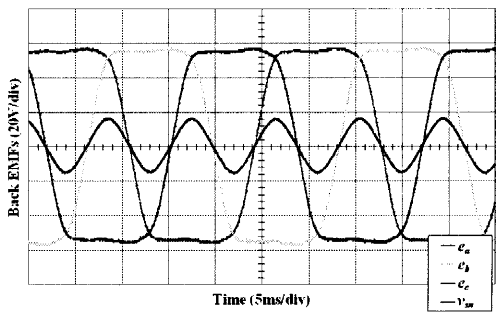

Fig. 2 Back-emf waveforms of 3-phase, 6-pole, 18-slot, BLDC motor

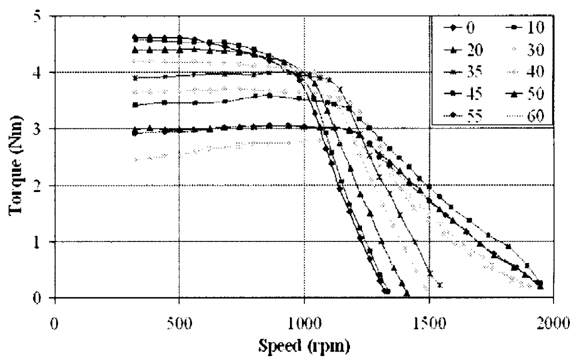

(a) Torque-speed curves for different commutation advance angles

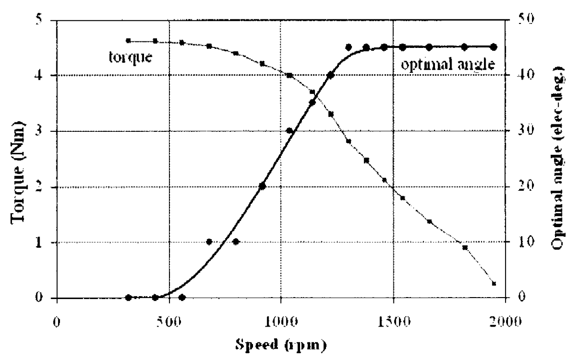

(b) Optimal commutation advance angle for maximum torque

Fig. 3 Torque-speed performance of BLDC motor

As can be seen, at low speed, the optimal commutation advance angle is zero, i.e. the phase current is in phase with the back-emf for maximum torque per ampere, Figure 4 (a). As can be seen, the phase current waveform is essentially rectangular, and the same as the demanded current $\tilde{i}_a$. However, above the base-speed the phase current which results with zero commutation advance is very much lower than the demanded current due to the increase in the back-emf, as shown in Figure 4 (b). With optimal commutation advance, however, the phase current can again be regulated to have an essentially rectangular waveform. However, at yet higher speeds in the flux-weakening mode, the phase current waveform deteriorates and becomes almost sinusoidal due to the influence of winding inductance since the higher order current harmonics are suppressed by their higher reactance as the speed increases, as shown in Figure 4 (c), in which it will also be noted that the peak-to-peak amplitude of the phase back-emf is significantly higher than the DC link voltage. When optimal commutation advance is employed, however, the maximum achievable output power increases to 450W which compares to 400W without commutation advance, as will be shown later, while the maximum speed increases from 1320rpm to 1950rpm.

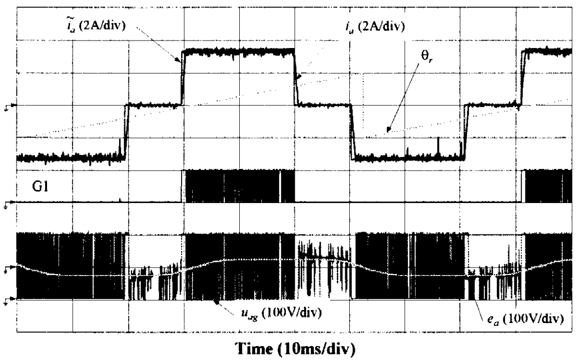

(a) Low speed, 320rpm, zero commutation advance

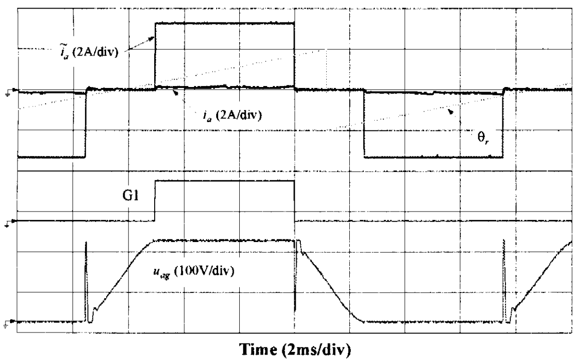

(b) 1320rpm, zero commutation advance

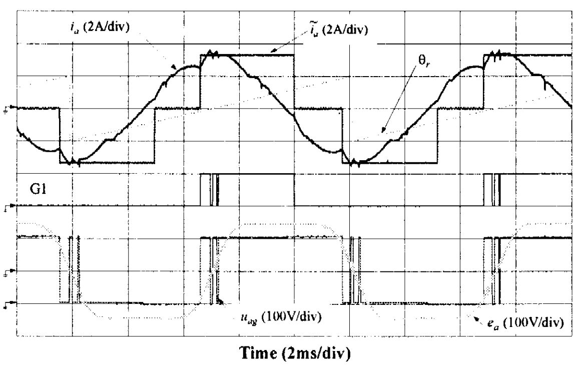

(c) 1950rpm, optimal commutation advance

Fig. 4 Measured waveforms in BLDC mode: rotor position (θ_r), reference phase current ($\tilde{i}_a$), actual phase current (i_a), inverter switching signal (G1), terminal voltage (u_{ag}), simulated back-emf (e_a)

4. FLUX-WEAKENING CONTROL AS BLAC DRIVE

Although the flux-weakening control of BLAC machines has been studied extensively [Zhu et al., 2003; Chan et al., 1994], generally it has been applied to machines which have an essentially sinusoidal back-emf waveform, not a trapezoidal waveform as is the case for the motor under consideration. It is easy to implement, since simple analytical equations exist for the optimal d- and q-axis currents, according to the speed and the motor parameters [Chan et al., 1994]. The maximum DC link voltage, $U_{max}=2U_{dc}/\pi$, is utilized in the flux-weakening mode. However, in order to compare the relative torque and speed capabilities when the motor under consideration is operated in BLDC and BLAC modes, both with and without optimal flux-weakening, the three criteria cited in section 2 are used to determine the phase current amplitude I_{max}, viz.: (a) the same electromagnetic torque is produced in the constant torque region in both BLDC and BLAC modes, (b) in both modes, the amplitude of the phase currents are the same, and (c) in both modes the copper loss, and, hence, the rms phase current is the same. The amplitude of the phase currents which corresponds to the foregoing conditions are given in Table 4.

Table 4 Amplitude of phase currents

Amplitude of phase current of BLDC motor (I_m)	Condition	Amplitude of phase current of BLAC motor (I_{max})
3.30 A	Same electromagnetic torque	3.56 A
	Same phase current amplitude	3.30 A
	Same RMS phase current	3.81 A

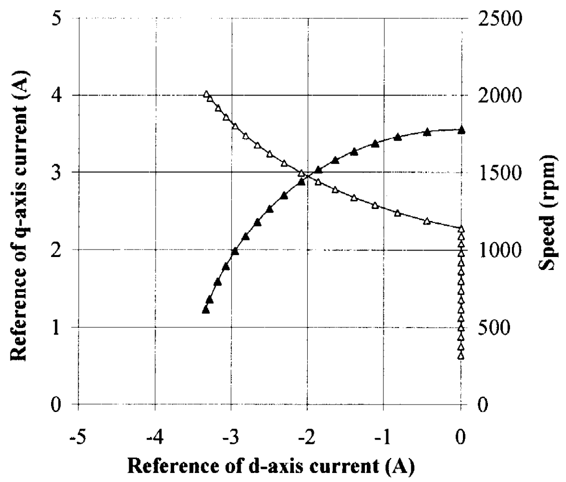

Fig. 5 Variation of optimal d-q axis current components with speed

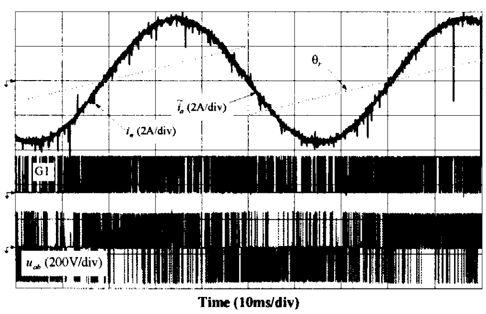

(a) 320rpm, without flux-weakening

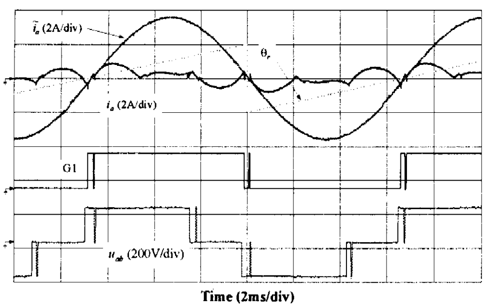

(b) 1480rpm, without flux-weakening

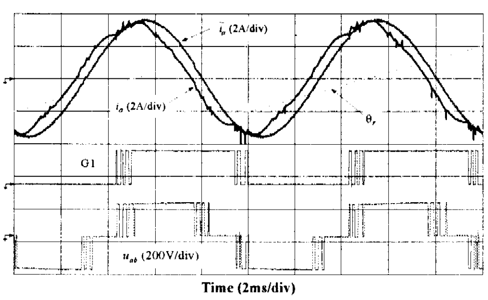

(c) 2010rpm, with optimal flux-weakening

Fig. 6 Measured waveforms in BLAC mode when I_{max}=3.56A.: rotor position (θ_r), reference phase current (i_a^*), actual phase current (i_a), inverter switching signal (G1), and terminal voltage (u_{ag})

Figure 5 shows the variation of the optimal d-and q-axis currents with speed, when I_{max}=3.56A. It can be seen from Figure 6 (a) and Figure 6 (b) that when flux-weakening control is not employed the phase current waveform is essentially sinusoidal when the motor operates below base-speed, but becomes very distorted above base-speed. However, with optimal flux-weakening control the phase current waveform is essentially sinusoidal throughout the speed range, Figure 6 (c), and, as can be seen from Figure 7 (a), the maximum attainable speed increases from ~1480rpm to ~2010rpm. Figure 7 also shows the measured maximum torque-speed curves which result when the motor is operated in BLDC and BLAC modes under the criteria which were cited earlier, viz. I_m = 3.30A, and I_{max}=3.56A, 3.30A and 3.81A, the performance being summarized in Table 5.

Table 5 Summary of performance when operated in BLDC and BLAC modes

Mode and phase current amplitude	Measured maximum torque	Measured max. speed With phase advance/ flux-weakening
BLDC, I_m=3.30A	4.6Nm	1950rpm
BLAC, I_{max}=3.56A (+9.6%)	4.6Nm	2010rpm
BLAC, I_{max}=3.30A	4.3Nm (-6.5%)	1940rpm
BLAC, I_{max}=3.81A (+15.5%)	5.0Nm (+8.7%)	2080rpm

Note: Values in ( ) are with reference to BLDC mode

5. COMPARISON OF BLDC AND BLAC MODES OF OPERATION

Figure 7 (a) shows the performance which is achieved when the amplitude of the idealized phase currents waveforms in BLDC and BLAC modes correspond to the same torque capability below base-speed, viz. 3.30A and 3.56A, respectively. As will be seen, above base-speed the torque and power which result in BLAC mode are significantly higher. This is that due to the influence of the winding inductance and back-emf harmonics on the current waveform in BLDC mode as they reduce the difference between supply voltage and the back-emf. Thus, for example, at the rated speed of 830rpm, while the phase current in BLAC mode is close to the reference value, in BLDC mode it is somewhat lower than the reference value. Figure 7 (b) shows the maximum torque/power-speed curves which result when the amplitude of the phase currents is the same in both BLDC and BLAC modes, viz. 3.30A. In this case, the phase current in BLAC mode is significantly reduced. Obviously, below base-speed, BLDC operation results in a higher output power for the same peak phase current.

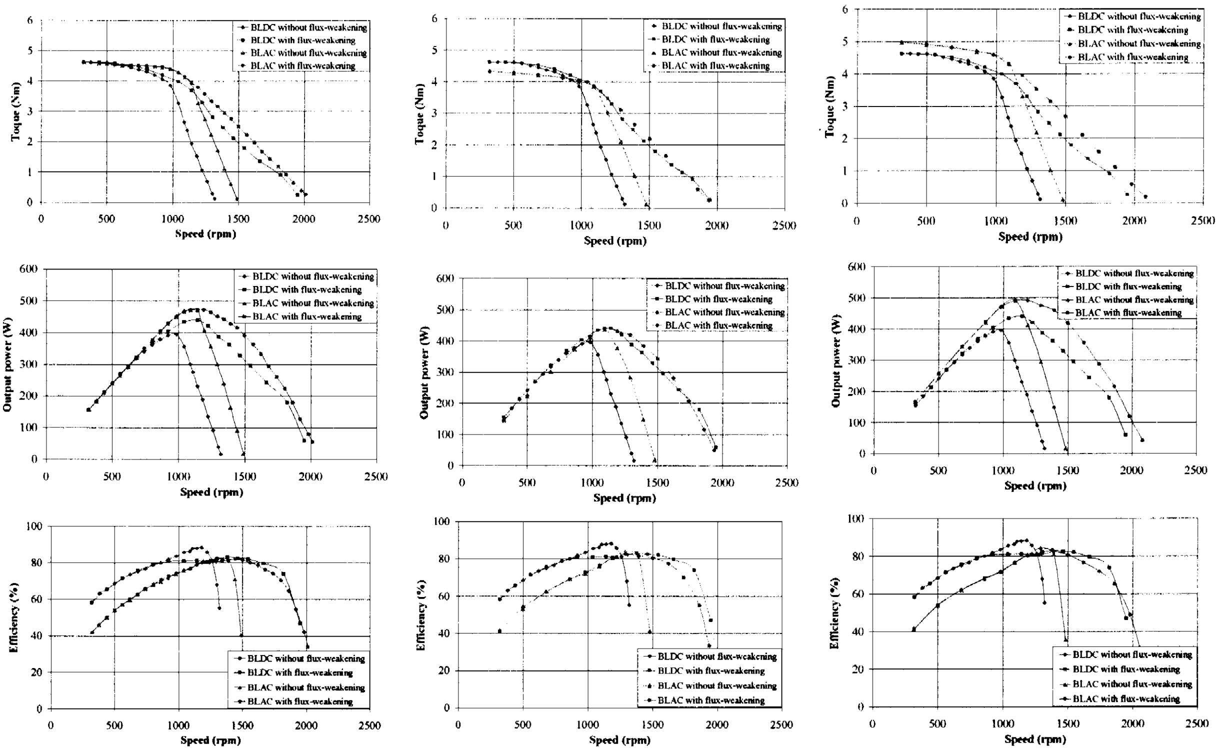

(a) Phase current amplitude in BLDC mode I_m=3.30A and in BLAC mode I_{max}=3.56A

(b) Phase current amplitude in BLDC mode I_m=3.30A, and BLAC mode I_{max}=3.30A

(c) Phase current amplitude in BLDC mode I_m=3.30A, and BLAC mode I_{max}=3.81A

Fig. 7 Performance comparisons when motor is operated in BLDC and BLAC modes

When flux-weakening is employed above base-speed, both BLDC and BLAC modes exhibit almost the same performance. Figure 7 (c) shows the maximum achievable torque/power-speed curves which result with the same RMS phase current in both BLDC and BLAC modes. As will be seen, the power and torque capability in the BLAC mode is significantly higher than that in BLDC mode. As can also be seen in Table 4, since the phase back-emf waveform of the motor under consideration does not have the ideal 120° elec. flat top which was assumed in the derivation of Table 2, the variation in the maximum torque capability with the mode of operation differs slightly from that which was predicted earlier.

In summary, the output power and torque of the BLAC operation in the flux-weakening region are greater than those of the BLDC operation in all three cases. However, as shown in Figure 7, it is found that for this particular motor and drive system, the BLDC operation generally has higher system efficiency below the base-speed in the constant torque region. Although this needs further investigation, the reasons for this are likely due to (a) the increased average torque contributed by the current harmonics in the BLDC operation, (b) the additional stator iron loss due to current harmonics in the surface-mounted magnet machine is relatively small, and (c) the reduced switching loss in the BLDC inverter, since switching loss occurs only in two phases of the BLDC drive if delta-modulated current regulation is used. However, the difference in efficiency becomes small in the flux-weakening region since the phase current waveform in the BLDC operation also becomes sinusoidal, while the number of switching becomes very low.

6. CONCLUSIONS

The performance of a permanent magnet brushless motor having a surface-mounted magnet rotor and an essentially trapezoidal back-emf waveform has been determined, when it is operated in both BLDC and BLAC modes in the constant torque and flux-weakening regions, assuming (a) the same torque, (b) the same peak current, (c) the same rms current. The results show that in the flux-weakening region the output power and torque in the BLAC mode are higher than those in the BLDC mode for all cases although the motor has a trapezoidal back-emf waveform. This should be considered for EV/HEV applications.

However, it should be recognized that while a permanent magnet brushless motor with a trapezoidal back-emf waveform can be operated in either BLDC or BLAC mode, other aspects of performance, in terms of torque ripple, should also be considered. Nevertheless, it is advantageous to operate such a motor in BLAC mode in the flux-weakening region, in terms of maximizing the torque and speed range.

References

Jahns, T. M., Flux-weakening regime operation of an interior permanent magnet synchronous motor drive, *IEEE Trans. Industry Applications*, Vol. 23, No. 4, 681-689, 1987.

Soong, W. L., and T. J. E. Miller, Field-weakening performance of brushless synchronous AC motor drives, *IEE Proc. -B*, Vol. 141, 331-340, 1994.

Zhu, Z. Q., Z. P. Xia, Y. F. Shi, D. Howe, A. Pride, and X. J. Chen, Performance of Halbach magnetised brushless ac motor, *IEEE Trans. Magnetics*, Vol. 39, No. 5, 2992-2994, 2003.

Chan, C. C., J. Z. Jiang, G. H. Chen, X. Y. Wang, and K. T. Chau, A Novel Polyphase Multipole Square-Wave Permanent Magnet Machine Drive for Electric Vehicles, *IEEE Trans. On Industry Applications*, Vol. 30, No. 5, 1258-1266, 1994.

Ishak, D., Z. Q. Zhu, and D. Howe, Permanent magnet brushless machines with unequal tooth widths and similar slot and pole numbers, *IEEE Trans. Industry Applications*, Vol. 41, No. 2, 584-590, 2005.

Ishak, D., Z. Q. Zhu, and D. Howe, Comparison of PM brushless motors, with either all or alternative wound teeth, *IEEE Trans. Energy Conversion*, Vol. 21, No.1, 95-103, 2006.

El-Refaie, A. M., and T. M. Jahns, Optimal flux weakening in surface PM machines using concentrated windings, *IEEE Trans. Industry Applications*, Vol. 41, No. 3, 790-800, 2005.

El-Refaie, A. M., T. M. Jahns, P. J. McCleer, and J. W. McKeever, Experimental verification of optimal flux weakening in surface PM machines using concentrated windings, *IEEE Trans. Industry Applications*, Vol. 42, No. 2, 443-453, 2006.

Zhu, Z. Q., and D. Howe, Influence of design parameters on cogging torque in permanent magnet machines, *IEEE Trans. on Energy Conversion*, Vol. 15, No. 4, 407-412, 2000.

Zhu, Z. Q., Y. S. Chen, and D. Howe, Iron loss in PM brushless ac machines under maximum torque per ampere and flux weakening control, *Trans. IEEE Magnetics*, Vol. 38, No. 5, 3285-3287, 2002.

Zhu, Z. Q., Y. S. Chen, and D. Howe, Comparison of iron losses in alternative permanent magnet brushless ac machines, *Proc. 16th Int. Conf. on Electrical Machines*, Vol. 2, 517-518, No. 234, 2004.

Atallah, K., D. Howe, P. H. Mellor, and D. A. Stone, Rotor Loss in permanent magnet brushless AC machines, *IEEE Trans. Industry Applications*, Vol. 36, No. 6, 1612-1618, 2000.

Ishak, D., Z. Q. Zhu, and D. Howe, Rotor eddy current loss in PM machines with fractional slot number per pole, *IEEE Trans.Magnetics*, Vol. 41, No. 9, 2462-2469, 2005.

Jahns, T. M., Torque production in permanent magnet synchronous motor drives with rectangular current excitation, *IEEE Trans. Industry Applications*, Vol. 20, No. 4, 803-813, 1984.

Safi, S. K., P. P. Acarnley, A. G. Jack, Analysis and simulation of the high-speed torque performance of brushless DC motor drives, *Proc. IEE -EPA*, Vol. 142, No. 3, 191-200, 1995.

Morimoto, S., M. Sanada, and Y. Takeda, Wide-speed operation of interior permanent magnet synchronous motors with high-performance current regulator, *IEEE Trans. Industry Applications*, Vol. 30, No. 4, 920-926, 1994.

Liu, Y., Z. Q. Zhu, and D. Howe, Direct torque control of PM brushless AC motors having non-sinusoidal back-emf waveforms, *Proc. 3rd Int. Conf. on Power Electronics, Machines, and Drives,* 425-429, 2006.

Zhu, Z. Q., Y. F. Shi, and D. Howe, Comparison of torque-speed characteristics of interior-magnet machine in brushless AC and DC modes for EV/HEV applications, *Journal of Asian Electric Vehicles*, Vol. 4, No. 1, 843-850, 2006.

(Received July 14, 2006; accepted September 30, 2006)